



Analysis of Piezoelectric Energy Harvester with Different Substrate Materials and Configurations

Fahmidul Huq Syed, Li Wah Thong^(✉), and Yee Kit Chan

Faculty of Engineering and Technology, Multimedia University, Melaka, Malaysia
lwthong@mmu.edu.my

Abstract. This paper presents the effect of different substrate materials and proof mass configurations through a simulation of a bimorph cantilever beam that consists of one-layer substrate material sandwiched between two layers of piezoelectric material (PZT-5A) to harvest the vibration energy. To evaluate the performance of the energy harvesting system within the range of 62 Hz to 80 Hz (except for the no tip mass condition), the tip mass will be relocated from the free end of the cantilever beam using a variety of proposed positions on the beam itself. The shape and sizes of the tip mass will also be varied accordingly to observe its impact on the performance of the system. In addition, a variety of different material applied as substrate material is being compared to observe its impact on the frequency response output. The material of the tip mass was also varied to analyse its differences. The simulation was done using COMSOL Multiphysics and the results was presented by varying the parameters of the model.

Keywords: Piezoelectric effect · Vibration energy harvesting · substrate materials · resonance frequency · cantilever beam

1 Introduction

The usage of natural vibration as a source of energy harvesting technologies has been one of the most widely researched sectors in the literatures over recent years. Vibration sources can be found in almost any parts of our daily life ranging from large infrastructures such as bridges, building, roads, and vehicles. Since the vibrational energy is easily obtainable in the ambient environment, harvesting and converting it into usable energy to power different small electric devices has been greatly evaluated over the years. Different methods were identified and successfully implemented by researchers in the literature. Generally, there are four methods applied for vibration-based energy harvesting including piezoelectric, electromagnetic, electrostatic and triboelectric transductions [1][2][3].

In the design of the energy harvesting system, the piezoelectric cantilever beam is commonly classified in two configurations, namely the unimorph and bimorph cantilever beam. The architecture of a bimorph energy harvester with proof mass is as shown in

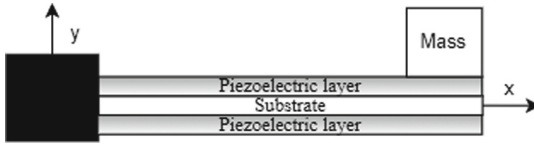


Fig. 1. Configuration of a bimorph piezoelectric cantilever beam [5]

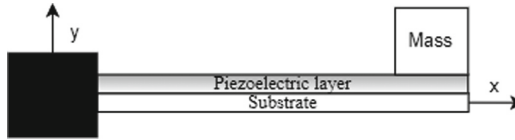


Fig. 2. Configuration of a unimorph piezoelectric cantilever beam [6]

Fig. 1. The bimorph piezoelectric cantilever beam includes an individual layer of a piezoelectric element linked to a layer of the nonpiezoelectric element, referred to as the ‘substrate layer’. Electrodes that accumulate the produced charges, are secured to the top and bottom surfaces of the piezoelectric element. The resonance frequency can be reduced by introducing extra mass onto the system, known as a tip/proof mass, at the free end of the beam. It is assumed that the piezoelectric based layout offers low voltage and current. Because of those bi-directional consequences, piezoelectric substances are broadly utilized for sensors and actuators. Piezoelectric substances are also utilized to produce electrical energy to drive electrical devices from the striking heels of shoes via walking or moving [4].

Figure 2 illustrates the configuration of a unimorph piezoelectric cantilever beam. The difference of this configuration to the bimorph system is the quantity of piezoelectric layer and its substrate material. Unlike bimorph cantilever beam, the substrate material for the unimorph system is not squeezed between two layers of piezoelectric material. The unimorph cantilever beams only contains of one layer of piezoelectric material and its substrate layer respectively.

2 Design of a Bimorph Cantilever Beam

2.1 Vibration Energy Harvesting Method

Conversion of vibration energy into electric power is a two-step concept. Initially, mechanical-to-mechanical converter is used to convert the vibration in a relative motion between two elements. Subsequently, the harvested mechanical vibration will be converted into electrical energy using mechanical-to-electrical converters such a piezoelectric materials or variable capacitors [7]. Among the electromagnetic, electrostatic and piezoelectric vibration energy harvesting techniques, the latter approach is widely preferred and applied prevalently because of its aptitude in harvesting vibration energy over a wide range of frequencies as well as its simple design and fabrication. Besides that, the piezoelectric energy harvester provides efficient energy conversion and real-time monitoring in comparisons with the other available methods [8][9][10].

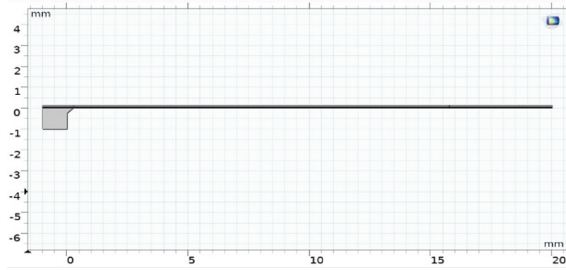


Fig. 3. The geometry of a bimorph cantilever beam without tip mass.

Table 1. Parameters of the piezoelectric cantilever beam without tip mass

Parameters	Values
Type of Beam	Bimorph
Piezoelectric layer material	Lead Zirconate Titanate (PZT-5A)
Substrate layer material	Several
Tip mass	Absent
Width of the beam	21 mm
Height of the beam	0.16 mm
Thickness of piezoelectric layer	0.06 mm
Thickness of substrate layer	0.04 mm

2.2 Parameters of Piezoelectric Cantilever Beam

To achieve significant outcomes from the simulation, few different setups of the bimorph cantilever beam was constructed in COMSOL Multiphysics by varying the location of the tip mass and the substrate material. To achieve the desired outcomes, many parameters have been defined depending on the variation of the setup. Figure 3 illustrates the first variation of the bimorph cantilever beam where the tip mass was excluded in the system. The simulation was solely done by changing the substrate materials and analysing the impact on its performance.

The parameters applied for the simulation of the piezoelectric cantilever beam is as shown in Table 1. Seven different materials were proposed for the variation of substrate layer in the configurations. Throughout the simulation, the piezoelectric layer remained the same and was set to be PZT-5A material. The properties of these materials are highlighted in Table 2. These properties are already built-in in COMSOL Multiphysics. Hence, they remained constant and no user defined parameters needed to be included.

In the second configurations, tip mass was added at the free end of the cantilever beam while the parameters of the cantilever beam were kept the same throughout its operation. The position and sizes of the tip mass was varied accordingly to observe its impact on the frequency response of the system. Figure 4 illustrate the different configurations of the tip mass placed on top of the cantilever beam. Table 3 describes the different

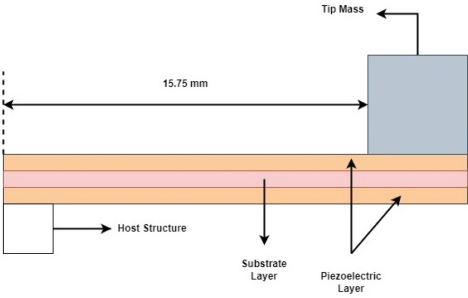
Table 2. Properties of the materials

Material	Properties	Values
Lead Zirconate Titanate (PZT-5A)	Young's Modulus (Pa)	66×10^9
	Density (kg/m^3)	7750
	Poisson's ratio	0.31
Structural Steel	Young's Modulus (Pa)	200×10^9
	Density (kg/m^3)	7850
	Poisson's ratio	0.30
Aluminum	Young's Modulus (Pa)	70×10^9
	Density (kg/m^3)	2700
	Poisson's ratio	0.33
Cast Iron	Young's Modulus (Pa)	140×10^9
	Density (kg/m^3)	7000
	Poisson's ratio	0.25
Copper	Young's Modulus (Pa)	110×10^9
	Density (kg/m^3)	8960
	Poisson's ratio	0.35
Tungsten	Young's Modulus (Pa)	411×10^9
	Density (kg/m^3)	19350
	Poisson's ratio	0.28
Lead	Young's Modulus (Pa)	16×10^9
	Density (kg/m^3)	11340
	Poisson's ratio	0.44
Nikel	Young's Modulus (Pa)	219×10^9
	Density (kg/m^3)	8900
	Poisson's ratio	0.31

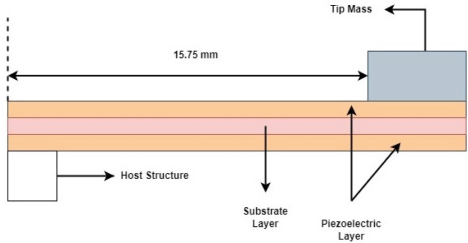
sizes and location of the tip mass applied on the cantilever beam in accordance to the configurations of A, B, C and D in Fig. 4. For each configuration of the tip mass, the substrate material of the cantilever beam was also varied accordingly using Table 2.

2.3 Simulation

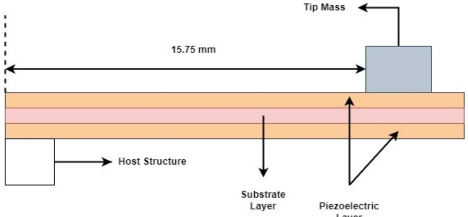
In the design and simulation of the piezoelectric energy harvesting system, COMSOL Multiphysics was applied as the main software to draw and simulate the performance of the system. A 2D model of the cantilever beam was drawn with the parameters mentioned in Table 1. A host structure was fixed on one end of the beam while the size,



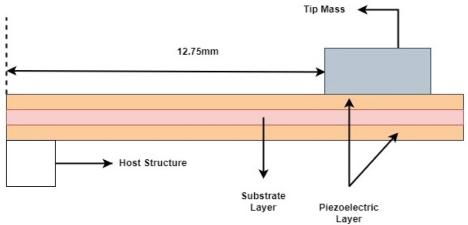
Configuration A



Configuration B



Configuration C



Configuration D

Fig. 4. Variety of tip mass on the cantilever beam

Table 3. Different Tip Mass Parameters

Parameters of tip mass	A	B	C	D
Width (mm)	4	4	2	4
Height (mm)	5.7	1.7	1.7	1.7
Distance from the host structure (mm)	15.75	15.75	15.75	12.75

shape, location and existence of the tip mass on the other free end was varied accordingly based on Fig. 4. Table 3 illustrates the changes of the tip mass parameters accurately.

Multiple boundary conditions were applied on the cantilever beam to achieve the potential outcome. For example, the mechanical damping at the hinged end of the beam was set to 0.001. The other end of the beam was kept under free conditions to allow displacement in the presence of vibration. These conditions were fixed for all the different cases proposed in this paper.

Likewise, in order to produce electrical power, a connection of a piezoelectric circuit was generated by using each of the piezoelectric layer as a terminal while using the hidden surfaces as ground. In concurrence with the electrostatics settings, electrical circuit settings had to be implemented too. This is to ensure that electrical responses can be obtained from the cantilever beam whenever there is mechanical vibration. The frequency range was set from 62 Hz to 80 Hz. This range of frequency has been set due to the potential use of piezoelectric harvesting system for harvesting energy in electric motor, which produces the similar range of vibration frequency [11]. However, a broader range of frequency, which is 160 Hz to 300 Hz was tuned for the no tip mass condition for comparison purposes of the resonance frequencies produced by each cantilever beams.

3 Results and Discussions

In order to analyse the performance of the cantilever beams in different configurations, the frequency response curves in terms of voltage and power were plotted accordingly and discussed based on its respective settings.

3.1 Cantilever Beam Without Tip Mass

The output of the simulation done in the absence of a tip mass did not show any peak performance with in the fixed range of 62–80 Hz and may not be suitable for harvesting energy in electric motors. Figure 5 shows that the peak voltages of all the specific materials are in a higher frequency range upon setting up a broader range of frequency between 160 Hz to 300 Hz. Aluminium reaches its highest voltage output of 1.41 V and power output of 0.08 mW at 219 Hz. At frequency of 204 Hz, cast iron produces a 1.55 V and 0.1 mW of voltage and power. Copper spikes optimum at 197 Hz with 1.61 V and 0.1 mW while Nickel provides a voltage and power output of 1.62 V and 0.11 mW at 199 Hz. Lead, Structural steel and Tungsten reaches their maximum output at 187 Hz, 202 Hz and 176 Hz respectively. Both the voltage and power outputs are shown in Fig. 5 and 6.

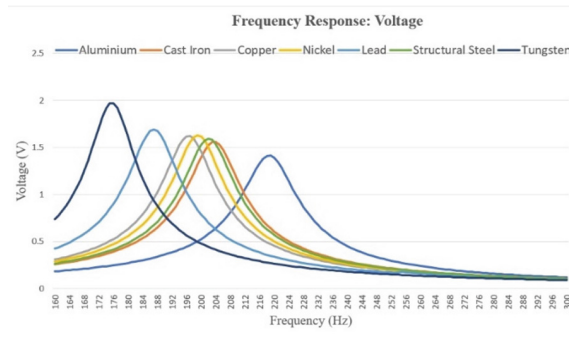


Fig. 5. Voltage output for no tip mass condition using different substrate materials.

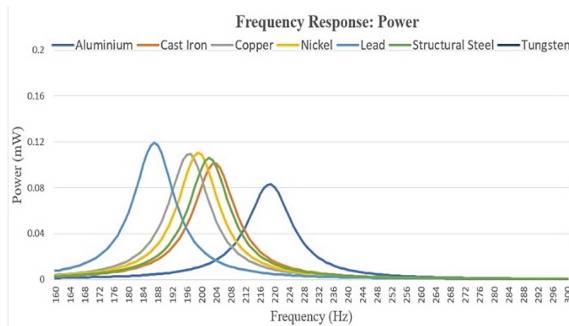


Fig. 6. Power output for no tip mass condition using different substrate materials.

3.2 Cantilever Beam with a Variety of Tip Mass Configurations

This section is divided into four subsections whereby the resultant frequency response output using the geometry and configuration of all the cases discussed in Fig. 3 are presented accordingly. As discussed earlier, the results will only focus on the frequency range of 62 Hz to 80 Hz for the application of the piezoelectric harvesting system in electric motor, which produces the similar range of vibration frequency.

3.2.1 Configuration A

In the first case, only Aluminium has shown some valid output compared to the other materials used within the applicable frequency range. As illustrated in Fig. 7 and Fig. 8, all the other material does not provide any voltage or power peaks within this range of frequency using this configuration. At the frequency of 64 Hz, Aluminium has showcased its optimum peak voltage of 5.63 V and power output of 1.33 mW. Further analysis on the graphs indicates that the other materials would show their optimum peak value at a frequency below 62 Hz. Thus, this configuration is only suitable for Aluminium as the substrate material in order to provide a valid output for the energy harvesting system.

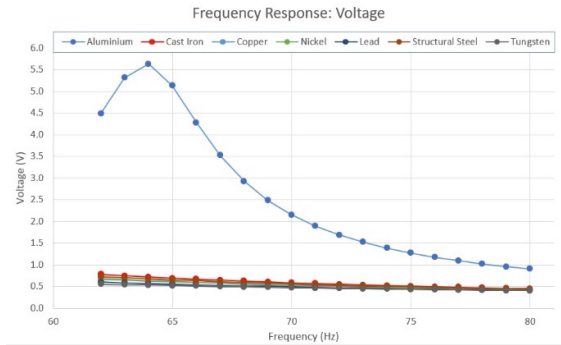


Fig. 7. Voltage Response Graph of Case A.

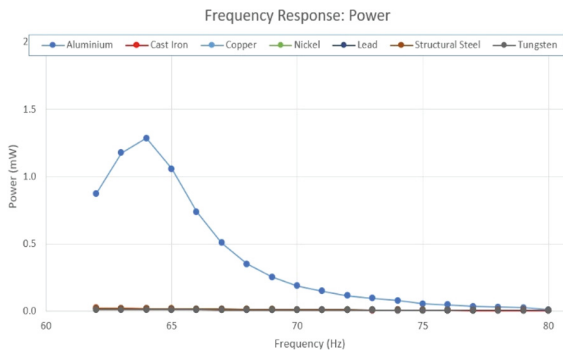


Fig. 8. Power Output Graph of Case A.

3.2.2 Configuration B

The setup of Case B has shown the most potential outcome among all the cases. The outputs of four different materials have broadly peaked at different range of frequencies as illustrated in Fig. 9. Copper and Nickel provides one of the highest peak voltage at the frequency of 66 Hz and 67 Hz respectively. From 65 Hz onwards, Copper shows another slightly more angular inclined peak, peaking at frequency of 66 Hz and then the peak decreases till frequency of 70 Hz, following the same curve during its incremental curve. From 70 Hz onwards, the decrease in both voltage and power are less stiff as the voltage is seen to reach 1.134 V while the power reaches at 0.1267 mW which is almost close to the flat line. Nickel displays the same outcome, but its highest peak happens at the frequency of 67 Hz, following the same pattern of peak down where its voltage and power dropping to 1.52 V and 0.05 mW at the frequency of 80 Hz.

Similarly, structural steel and cast iron exhibit the same frequency response output except structural steel tops at the frequency of 71 Hz with 5.242 V and 1.127 mW of voltage and power output respectively while the cast iron produces peak voltage and power of 4.8 V and 0.952 mW respectively at frequency of 74 Hz. No promising results were observed for the other materials as shown in Fig. 9 and Fig. 10.

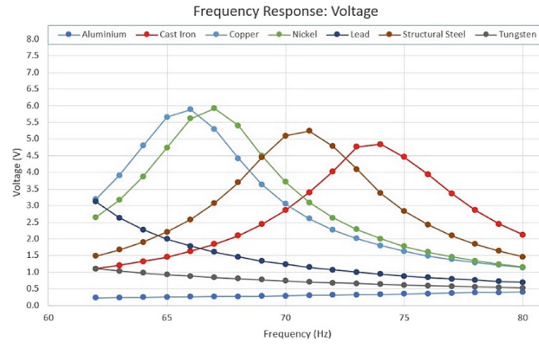


Fig. 9. Voltage Response Graph of Case B.

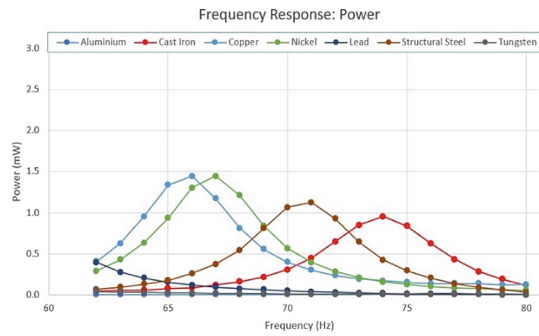


Fig. 10. Power Output Graph of Case B

3.2.3 Configuration C

In terms of configuration C, the tip mass was reduced to half the size in comparison with the configuration B. The distance of the mass remains the same as previous configurations. Based on the frequency response curves shown in Fig. 11 and Fig. 12, only the Lead material shows the prominent peak voltage and power results within the range of frequency. Aluminium is laid in the bottom of the chart as it did not show any spike in the power output while astonishingly, Tungsten shows quite spiked up results at the beginning and then the spike declines pretty gradually to zero without showing any other spike up for the rest of the frequency.

Cast Iron and Structural Steel displays similar results and so does Copper and Nickel. The similarity among these four materials is that they show an increment of their power output spike within the range of 75–80 Hz. This increment seems to be larger when Copper and Nickel were used respectively. For the rest of the two materials the spike is quite marginal to the zero line. The inclination of the curve of the voltage for these four materials also show a pattern that their spike increases within the 70–75 Hz range and from 76–80 Hz the spike is more rapid. It is predicted that these materials may show better spikes if the frequency range is extended.

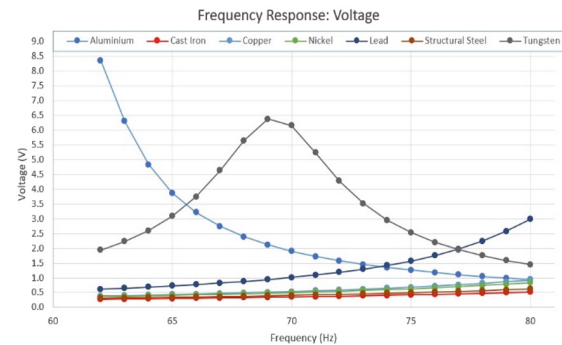


Fig. 11. Voltage Response Graph of Case C.

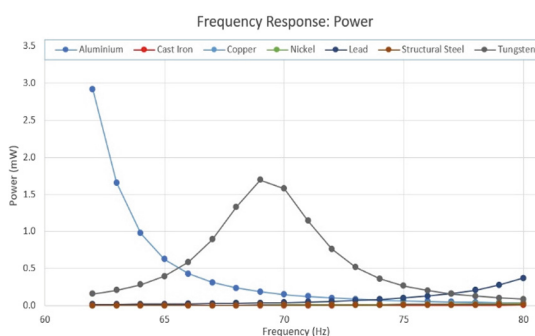


Fig. 12. Power Output Graph of Case C.

3.2.4 Configuration D

For this setup, similar tip mass as Configuration B was applied except the tip mass will be placed nearer to the fixed end of the cantilever beam. This configuration is done to observe the impact of the tip mass on different location on the cantilever beam. Figure 13 and Fig. 14 illustrates that only the Lead material is able to produce the highest peak output on the resonance frequency of 74 Hz with a voltage and power response of 6.4 V and 1.7 mW respectively. At the beginning of the graph, Tungsten has a very high peak for both of its voltage and power resulting in 8.3 V and 2.9 mW respectively, which decreases rapidly till the frequency of 65 Hz. From the observation, Tungsten may have a higher peak voltage at frequency below 62 Hz.

Copper, Nickel, Structural steel and Cast iron (Higher to lower) showcases a gradual increase of the line as they surpass 75 Hz. It is plausible that these materials may show better results for a higher range of frequency. Thus, for this configuration, these materials will work better for vibration in higher range of frequency output for the energy harvesting system. Conclusively, the Lead material works the best in this configuration for harvesting vibrational energy ranging from 70 Hz to 80 Hz applications.

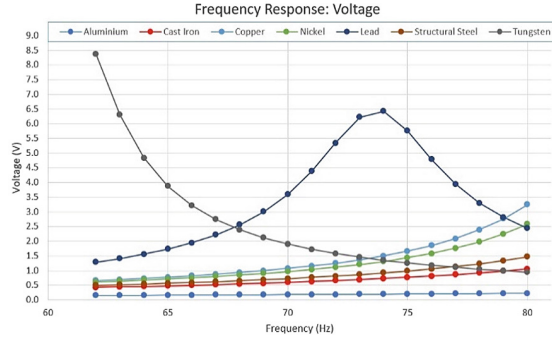


Fig. 13. Voltage Response Graph of Case D.

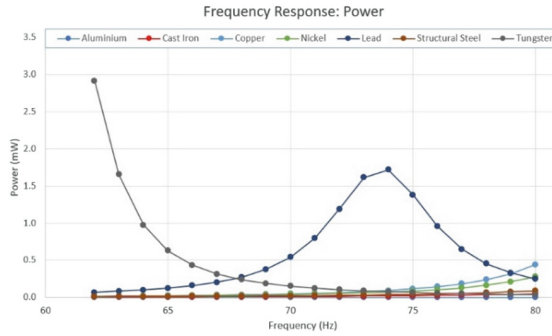


Fig. 14. Power Output Graph of Case D.

3.3 Cantilever Beam with a Variation of Tip Mass Material

This section is divided into four subsections whereby the resultant frequency response output using different tip mass material such as Cast Iron, Copper, Nickel and Structural Steel are presented accordingly. In each of these subsections, the material of the tip mass is kept the same as the substrate materials changes accordingly in order to evaluate its impact on the energy harvesting system. The configuration of Case B has been adopted for this study since it produces the best case scenario in the previous work.

3.3.1 Cast Iron as Tip Mass Material

Figure 15 and Fig. 16 shows the frequency response curves in terms of voltage and power output respectively for the simulation of all the substrate materials when cast iron material was used as the tip mass. Based on the observation, Tungsten shows the highest value of 5.23 V and 1.15 mW at the frequency of 74 Hz. Lead reaches its maximum peak at frequency of 72 Hz with voltage peak of 4.9 V and power peak of 1.04 mW. The other materials show quite similar and competitive values on their voltage and power curves whereby Aluminium, Nickel and Structural Steel produces similar frequency response curves with voltage peak of 4.9 V at the resonance frequency of 74 Hz. Copper substrate

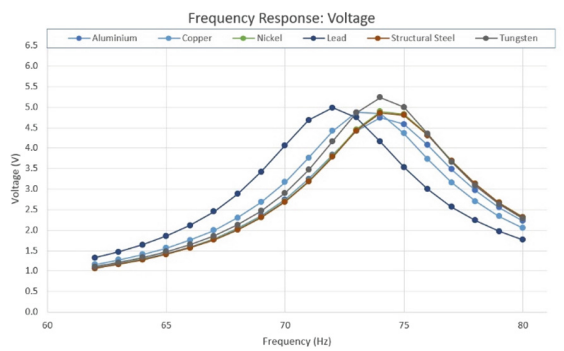


Fig. 15. Voltage Response of Different Materials using Cast Iron Tip Mass

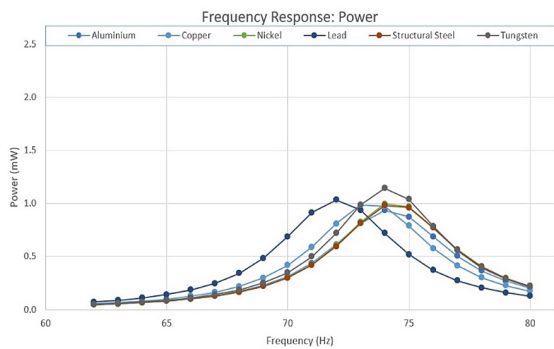


Fig. 16. Power Response of Different Materials using Cast Iron Tip Mass

also produces peak voltage of 4.9 V except at a different resonance frequency of 73.5 Hz. In terms of power output, these four substrate materials give the power output of 0.9 mW at its respective resonance frequencies as shown in Fig. 16.

3.3.2 Copper as Tip Mass Material

The resultant frequency response output when copper is used as the material of the tip mass yield similar but lower output voltage and power in comparison with the Cast Iron tip mass variation. The difference is that the voltage peak for different substrate materials occurs between the frequency of 64 Hz to 68 Hz. Lead produces a peak value in voltage and power of 5.8 V and 1.4 mW respectively at frequency of 65 Hz while Tungsten surpasses 6 V margin and 1.59 mW at the frequency of 67 Hz. Nickel and Structural Steel produces almost similar curves with peak voltage of 5.8 V at resonance frequency of 67 Hz. Similarly, Aluminium and Cast Iron behaves in the same pattern with peak voltage of 5.9 V at the frequency 66 Hz. In comparison with other materials of tip mass, the voltage and power output by this variation is one of the highest within the range above 5.8 V and 1.4 mW respectively (Figs. 17 and 18).

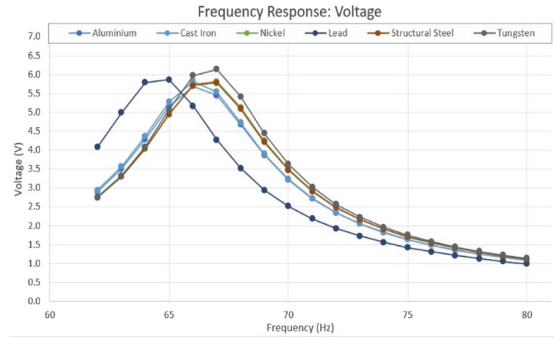


Fig. 17. Voltage Response of Different Materials using Copper Tip Mass

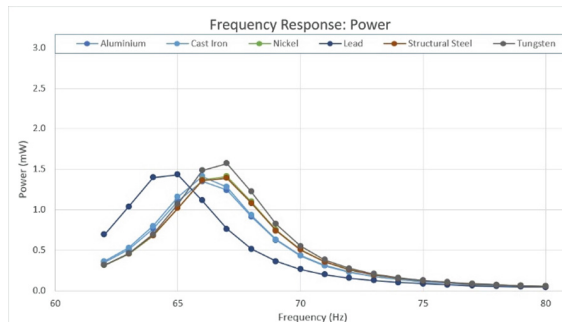


Fig. 18. Power Response of Different Materials using Copper Tip Mass

3.3.3 Nickel as Tip Mass Material

The frequency response for both the voltage and power output of the system that uses Nickel as a tip mass yields similar pattern as the results in the previous case where Copper is applied as the tip mass. Both of these materials provides similar peak voltages which is marginally different in decimal points. In this configuration, Lead produces a peak voltage and power of 5.9 V and 1.46 mW respectively at the frequency of 65 Hz. Similarly, Tungsten has its upmost peak at resonance frequency of 67 Hz producing voltage peak of 6.16 V and power peak of 1.605 mW. Aluminium, Nickel and Structural Steel shares the same resonance frequency of 66 Hz with voltage peak at 5.8 V, 5.6 V and 5.5 V respectively. Cast Iron produces voltage peak of 5.9 V at the frequency of 66 Hz which is similar results as the Copper tip mass configurations. The vast similarity in both these cases can be seen in Fig. 19 and Fig. 20 respectively. In terms of power output, similar pattern was observed at the respective resonance frequency of each different substrate material. Based on the observation, the change of the tip mass material for both of the Copper and Nickel tip mass variations has little impact on the selection of the substrate material.

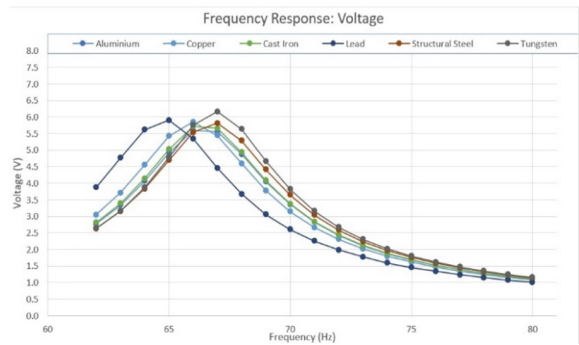


Fig. 19. Voltage Response of Different Materials using Nickel Tip Mass

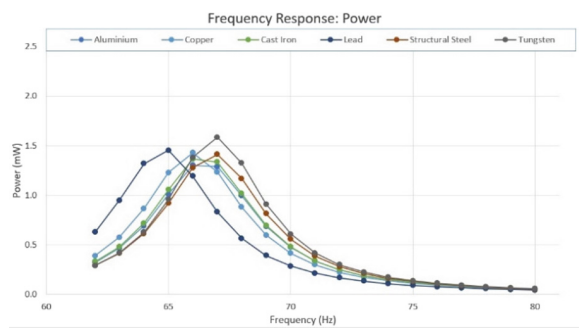


Fig. 20. Power Response of Different Materials using Nickel Tip Mass

3.3.4 Structural Steel as Tip Mass Material

The results of each substrate material for structural tip mass configurations are quite competitive as shown in Fig. 21 and Fig. 22. Similar to the previous cases, the most elevated values are gained when Tungsten is used as the substrate material. At the frequency of 70 Hz, Copper, Cast Iron and Aluminium reaches their highest peak voltage valuing at 5.33 V, 5.24 V, and 5.10 V respectively. Aluminium produces the lowest peak voltage among all the other materials. Lead and Nickel both reaches their optimum peak voltage of 5.32 V at the resonance frequency of 69 Hz and 71 Hz respectively. Both Lead and Nickel produces similar pattern in its power output with the peak power of 1.192 mW and 1.195 mW respectively. In comparison with other materials of tip mass, the resultant frequency response curves produce slightly lower voltage and power output.

3.4 Summary of Obtained Results

The following table show results obtained by Tungsten, Copper and Aluminium within the range of their resonance frequency for the case where structural steel has been used as the tip mass material. Hopefully this case would be sufficient to validate the elaboration on behalf all the cases where different materials have been used as they have shown similarity in the pattern of the outputs.

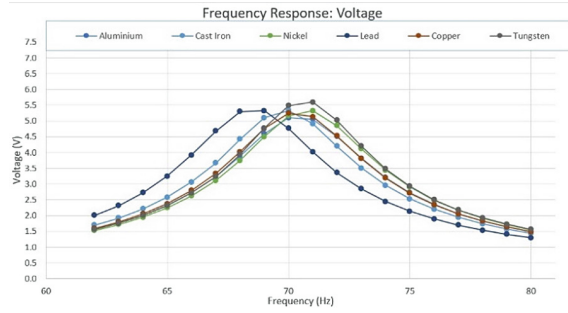


Fig. 21. Voltage Response of Different Materials using Structural Steel Tip Mass

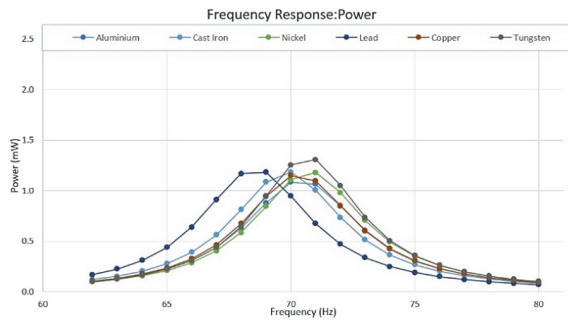


Fig. 22. Power Response of Different Materials using Structural Steel Tip Mass

Table 4. Obtained voltage and power outputs by using Structural steel as a tip mass material (Tungsten, Copper, Aluminium)

Frequency (Hz)	Structural Steel					
	Tungsten		Copper		Aluminium	
	(V)	(mW)	(V)	(mW)	(V)	(mW)
67	3.243446	0.438331	3.672941	0.562104	3.231403	0.435082
68	3.941785	0.647403	4.419249	0.81374	3.882345	0.628025
69	4.77116	0.948499	5.103439	1.085212	4.592887	0.878942
70	5.488066	1.254953	5.330338	1.183854	5.101451	1.084367
71	5.601679	1.30745	4.912025	1.005333	5.056245	1.065234
72	5.019476	1.049798	4.199306	0.734757	4.509421	0.847286
73	4.200251	0.735088	3.509026	0.513053	3.814515	0.606272

3.5 Discussion

One of the advantages of piezoelectric material is that the range of frequency is broader than other means of energy harvesting methods. However, in this study, we have kept our range quite minimum which in some cases have shown us half of the scenario. If

we look at all four cases where we have used different materials as the tip mass, the similarity is all the other materials have shown a resonance within a very nearby margin of frequency. As illustrated in Table 4, two out of three materials have resonated at 70 Hz. The theory of the resonance of these tip mass materials is related to their density. Heavier the material, lower their resonance frequency. Referring to Table 2, Tungsten has the highest density among all the material and its resonance is below 62 Hz which is the initial range of our study hence the results of Tungsten as a tip mass material has not been displayed. Similarly, Aluminium has the lowest density among all, and all the substrate materials have resonated above 100 Hz while Aluminium has been used as the tip mass hence again the results have not been displayed due to it being out of the range of our study. Copper and Nickel have a very minimum margin of difference in their density; hence they project similar results throughout the whole study. It is not only that the density of the material affects the resonance frequency, it also affects the magnitude of the results. Heavier the material, larger the magnitude of the output. If we just focus on the output produced by Tungsten while using different tip mass materials, the whole scenario gets clarification. Among all the four cases of different tip mass materials discussed above, Copper has the highest density and the results obtained while using Copper as a tip mass material are bigger in magnitude than the rest of the materials.

As well as the cases that study the difference in shape concludes into showing that, bigger the tip mass higher the output in a lower frequency.

As we lay down all the facts gathered from the scrutiny of the study, it does not point us to one superior material than others. If we use Copper or Nickel as a tip mass material it would show us the best results within the margin of 65–67 Hz, but if the application or device requires peak at higher frequencies, above 70 Hz per say, Cast Iron would provide better results. The whole advantage of the output gained from the study is that it allows to pick materials based on the requirement of the application, device, or product.

4 Conclusion

This paper presents a comprehensive study on the frequency response output in terms of voltage and power output using different tip mass configurations and a variety of materials as the substrate layer. Multiple configurations of geometry and several materials have been used in the bimorph cantilever beam to inspect the results. Based on the analysis of the outcomes, it is safe to say that all the materials used in the study show prominent outcomes at different stages. The outcomes are co-related to the properties of the materials. Announcing the best option of configuration and material would be vague as it completely depends on the requirement. However, it is found that the outcome can be manipulated by using different shape of the tip mass, different location on the beam and also by the selection of the materials. In addition, the results could also be enhanced by changing the length-width ratio [12]. Some of the materials portrayed the possibility of showing better worth in a broader range of frequency.

Acknowledgments. This work was supported by the Ministry of Higher Education of Malaysia under the Fundamental Research Grant Scheme (FRGS/1/2020/TK0/MMU/03/13). The authors would also like to acknowledge the Faculty of Engineering and Technology, Multimedia University for the support given in conducting this research.

Authors' Contributions. F.H.S., L.W.T. and Y.K.C. contributed to the design and implementation of the research, to the analysis of the results and to the writing of the manuscript.

References

1. R. Ahmed, F. Mir, and S. Banerjee, "A review on energy harvesting approaches for renewable energies from ambient vibrations and acoustic waves using piezoelectricity," *Smart Mater. Struct.*, vol. 26, no. 8, p. 085031, 2017. doi: <https://doi.org/10.1088/1361-665x/aa7bfb>.
2. J. Chen, Q. Qiu, Y. Han, and D. Lau, "Piezoelectric materials for sustainable building structures: Fundamentals and applications," *Renew. Sustain. Energy Rev.*, vol. 101, pp. 14–25, 2019. doi: <https://doi.org/10.1016/j.rser.2018.09.038>.
3. A. Mohanty, S. Parida, R. K. Behera, and T. Roy, "Vibration energy harvesting: A review," *J. Adv. Dielectr.*, vol. 9, no. 4, pp. 1–17, 2019. doi: <https://doi.org/10.1142/S2010135X1900019>.
4. K. Fan, Z. Liu, H. Liu, L. Wang, Y. Zhu, and B. Yu, "Scavenging energy from human walking through a shoe-mounted piezoelectric harvester," *Appl. Phys. Lett.*, vol. 110, pp. 143902, 2017. doi: <https://doi.org/10.1063/1.4979832>.
5. E. A. Abbasi, A. Allahverdizadeh, R. Jahangiri, and B. Dadashzadeh, "Design and Analysis of a Piezoelectric-Based AC Current Measuring Sensor," *International Journal of Mechanical and Mechatronics Engineering*, vol. 11, no. 10, pp. 1666–1671, 2017. doi: <https://doi.org/10.5281/zenodo.1132447>.
6. H. Li, C. Tian, and Z. D. Deng, "Energy harvesting from low frequency applications using piezoelectric materials," *Appl. Phys. Rev.*, vol. 1, no. 4, 2014. doi: <https://doi.org/10.1063/1.4900845>.
7. N. Chen, H. J. Jung, H. Jabbar, T. H. Sung, and T. Wei, "A piezoelectric impact-induced vibration cantilever energy harvester from speed bump with a low-power power management circuit," *Sensors Actuators A Phys.*, vol. 254, pp. 134–144, 2017. doi: <https://doi.org/10.1016/j.sna.2016.12.006>.
8. Z. Zhang, H. Xiang, Z. Shi, and J. Zhan, "Experimental investigation on piezoelectric energy harvesting from vehicle-bridge coupling vibration," *Energy Convers. Manag.*, vol. 163, pp. 169–179, 2018. doi: <https://doi.org/10.1016/j.enconman.2018.02.054>.
9. A. Karami, Di. Galayko, and P. Basset, "A Novel Characterization Method for Accurate Lumped Parameter Modeling of Electret Electrostatic Vibration Energy Harvesters," *IEEE Electron Device Lett.*, vol. 38, no. 5, pp. 665–668, 2017. doi: <https://doi.org/10.1109/LED.2017.2682232>.
10. Y. Pei, Y. Liu, and L. Zuo, "Multi-resonant electromagnetic shunt in base isolation for vibration damping and energy harvesting," *J. Sound Vib.*, vol. 423, pp. 1–17, 2018. doi: <https://doi.org/10.1016/j.jsv.2018.02.041>.
11. P. V. Malaji and S. F. Ali, "Analysis of energy harvesting from multiple pendulums with and without mechanical coupling," *Eur. Phys. J. Spec. Top.*, vol. 224, no. 14–15, pp. 2823–2838, 2015. doi: <https://doi.org/10.1140/epjst/e2015-02591-7>.
12. W. P. Q. Tong, B. M. S. Muhammad Ramadan, and T. Logenthiran, "Design and Simulation of a Piezoelectric Cantilever Beam for Mechanical Vibration Energy Harvesting," In: *Int. Conf. Innov. Smart Grid Technol. ISGT Asia 2018*, pp. 1245–1250, 2018, doi: <https://doi.org/10.1109/ISGT-Asia.2018.8467796>.

Open Access This chapter is licensed under the terms of the Creative Commons Attribution-NonCommercial 4.0 International License (<http://creativecommons.org/licenses/by-nc/4.0/>), which permits any noncommercial use, sharing, adaptation, distribution and reproduction in any medium or format, as long as you give appropriate credit to the original author(s) and the source, provide a link to the Creative Commons license and indicate if changes were made.

The images or other third party material in this chapter are included in the chapter's Creative Commons license, unless indicated otherwise in a credit line to the material. If material is not included in the chapter's Creative Commons license and your intended use is not permitted by statutory regulation or exceeds the permitted use, you will need to obtain permission directly from the copyright holder.

